HAL
open science

Analysis of micro-dispersed PCM-composite boards behavior in a buiding's wall for different seasons

Kamal El Omari, Yves Le Guer, Pascal Bruel

To cite this version:

Kamal El Omari, Yves Le Guer, Pascal Bruel. Analysis of micro-dispersed PCM-composite boards behavior in a buiding's wall for different seasons. Journal of Building Engineering, 2016, 7, pp.11. 10.1016/j.jobe.2016.07.013 . hal-01353957

HAL Id: hal-01353957

https://inria.hal.science/hal-01353957

Submitted on 20 Apr 2024

HAL is a multi-disciplinary open access archive for the deposit and dissemination of scientific research documents, whether they are published or not. The documents may come from teaching and research institutions in France or abroad, or from public or private research centers.

L'archive ouverte pluridisciplinaire **HAL**, est destinée au dépôt et à la diffusion de documents scientifiques de niveau recherche, publiés ou non, émanant des établissements d'enseignement et de recherche français ou étrangers, des laboratoires publics ou privés.

Author's Accepted Manuscript

www.elsevier.com/locate/jobe

Analysis of micro-dispersed PCM-composite boards behavior in a building's wall for different seasons

Kamal EL OMARI, Yves LE GUER, Pascal BRUEL

PII: S2352-7102(16)30111-5
DOI: http://dx.doi.org/10.1016/j.jobe.2016.07.013
Reference: JOBE161

To appear in: *Journal of Building Engineering*

Received date: 2 February 2016
Revised date: 11 May 2016
Accepted date: 31 July 2016

Cite this article as: Kamal EL OMARI, Yves LE GUER and Pascal BRUEL Analysis of micro-dispersed PCM-composite boards behavior in a building's wal for different seasons, *Journal of Building Engineering* http://dx.doi.org/10.1016/j.jobe.2016.07.013

This is a PDF file of an unedited manuscript that has been accepted fo publication. As a service to our customers we are providing this early version o the manuscript. The manuscript will undergo copyediting, typesetting, an review of the resulting galley proof before it is published in its final citable form Please note that during the production process errors may be discovered whic could affect the content, and all legal disclaimers that apply to the journal pertain

Analysis of micro-dispersed PCM-composite boards behavior in a building's wall for different seasons

Kamal EL OMARI[a,*], Yves LE GUER[a], Pascal BRUEL[b]

[a] *Université de Pau et des Pays de l'Adour (UPPA), Laboratoire des Sciences de l'Ingénieur Appliquées à la Mécanique et au génie électrique (SIAME), 64000 Pau, France.*

[b] *CNRS - Laboratoire de Mathématiques et de leurs Applications, Inria Cagire Team, 64000 Pau, France.*

Abstract

The integration of phase change materials (PCMs) in buildings especially in their walls is the subject of more than a decade of growing interest due to their potentialities for energy saving and enhancement of thermal comfort. The present investigation concerns the applications related to thermal insulation. The idealized composite wall considered here numerically can be thought of as resulting from the incorporation of shape-stabilized PCM particles in a polymer matrix. A novel model is developed to study the thermal behavior of this PCM-composite when used as a planar insulating material submitted to variable thermal modulations on one of its faces. The numerical model couples the heat transfer in the wall with the heat transfer and the crystallization/melting process within PCM inclusions considered as spherical. Both processes are modeled by a finite volume approach combined with the enthalpy method to account for the phase change. Simulation results are used to monitor the temperatures in the wall and quantify the energy exchanges between its two sides. The thickness of the wall and the volume fraction of the incorporated PCM were varied in this study. This analysis permits to point out the configurations for which the negative effect of the higher thermal conductivity of the PCM outweighs the benefits related to its latent heat. The analysis is extended to different external temperature modulations representing different typical seasons/climates. The results show the impact of the choice of the PCM phase change temperature on the wall thermal efficiency over the year. For the case investigated, it was shown that a PCM composite board with increased performances during a summer day exhibits a degraded behavior during a winter day when compared to a pure (without PCM) insulation material.

*Corresponding author.

Email address: `kamal.elomari@univ-pau.fr` (Kamal EL OMARI)

Keywords: Phase change material (PCM), composite board, dispersed PCM, building thermal insulation, enthalpy method.

1. Introduction

It is widely accepted that buildings and particularly those dedicated to housing represent a significant potential for energy saving, mainly related to the use of heating and air conditioning systems [1, 2, 3]. In that domain, the objective of the research and development community is to develop innovative approaches to save energy while preserving if not enhancing the thermal comfort of the buildings' inhabitants. In that framework, quite a significant number of recent studies focused on the use of phase change materials (PCMs) in buildings. They can be used as standalone systems to store energy, embedded in the structure [4, 5, 6] or in the external envelope [7, 8, 9]. The integration of PCMs results in an increase of the building thermal inertia, especially for lightweight construction. Combined with an efficient insulating material, it helps to reduce the indoor temperature peaks related to the outdoor temperature evolution and the solar radiation received at the external facades. Different techniques allow the integration of PCMs in building envelope materials: impregnation, incorporation of micro-encapsulations or macro-encapsulation in the form of slabs for example [10, 11, 12]. These solutions have attracted a great interest and have been the subject of a significant number of both numerical and experimental studies [13, 14, 15, 16, 17, 18]. There exist also encapsulation free techniques based on the direct incorporation of the PCM during the fabrication process or on immersion methods for natural porous materials [19]. For PCM-composite boards based on natural polymer matrices, one promising method involves the use of the low-energy emulsification technique [20, 21]. Since the plain insulation panels e.g. PCM-free commercially available have standardized thicknesses, the development of a PCM-composite board offering the same thickness range seems a reasonable choice. But even the choice of the proper PCM to be incorporated in a given matrix is not straightforward though. First, because of its relatively high conductivity when compared to that of the matrix, the overall thermal behavior of the PCM-composite board may be degraded under certain conditions when compared to that of its PCM free counterpart. Second, a melting temperature suitable for high outdoor temperatures (e.g. summer days) may lead to poor performances for lower external temperatures (e.g. winter days). Since a case by case analysis will ultimately

discriminate between the possible combinations of parameters, the availability of physical models that permits to discriminate a priori between the different possible alternatives is highly desirable. Accordingly, the goal of the present study is to propose such a numerical model and to illustrate for generic situations how it can be used to analyze the overall thermal effectiveness of a PCM-composite board and compare it with that of a plain board of the same thickness. This contribution is organized as follows: first, the proposed model and the method of solution are presented and validated. Then, the model is applied to the academic configuration of a harmonic external temperature modulation around the melting temperature chosen equal to the indoor temperature. The sensitivity to the nature of the insulating matrix is investigated by considering a more conductive material (i.e. cement). The case of a non-smooth harmonic modulation of the outdoor temperature is also investigated to evidence the effect of small-scale perturbations. Finally, the results obtained for a more realistic but still idealized external temperature evolution representative of either a summer or winter generic day are discussed.

2. Numerical Modelling

2.1. Physical model and assumptions

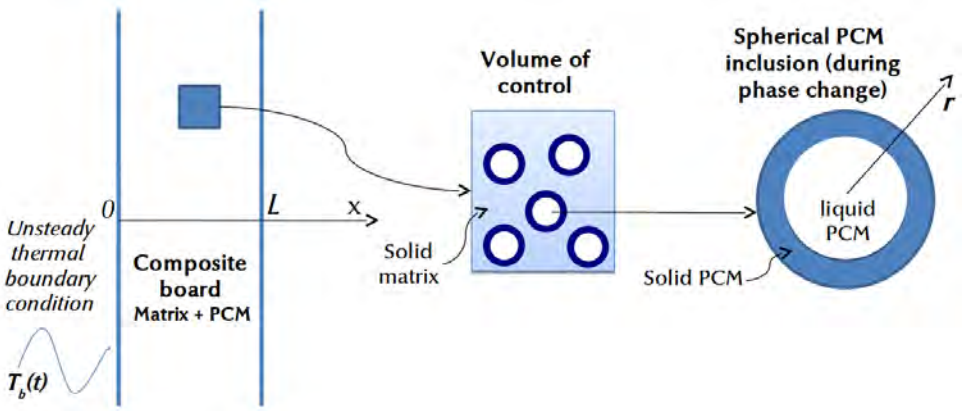

Figure 1: *Sketch of the modelled system: the composite board and a volume of control containing PCM spheres undergoing phase change.*

The unsteady thermal behavior of an insulation board containing microscopic spherical inclusions of a PCM is investigated. The diameter of the monodisperse PCM particles is $d = 100$ μm [21]. The PCM spheres are homogeneously dispersed in a solid matrix (see Fig. 1). The wall has a relatively small thickness compared to its lateral dimensions

which allows us to use a one-dimensional model for the heat transfer through it. The heat transfer model considers thermal conduction in the matrix and thermal conduction inside the PCM inclusions along with melting and crystallization phenomena combined with an appropriate boundary condition at the interface. As the inclusions are small in diameter (100 μm), the natural convection inside these PCM inclusions is not taken into account when they are in liquid state (i.e. the Rayleigh number is well below 1). In the equation of heat governing the thermal transfer in the wall, appears a source term Φ_i corresponding to the power exchanged between the solid matrix and the PCM spheres, namely:

$$\int_{V_i} (1-\phi)(\rho c_p)\frac{\partial T}{\partial t}\mathrm{d}V = \int_{S_i} k_{\mathrm{eff}}\vec{\nabla}T \cdot \vec{\mathrm{d}}S + \Phi_i \tag{1}$$

where V_i is a control volume within the matrix surrounded by a surface S_i. ϕ is the volume fraction of PCM contained in a control volume V_i. The source term Φ_i representing the heat flux exchanged between the spheres and the matrix of volume $(1-\phi)V_i$ is detailed below. The effective thermal conductivity of the composite k_{eff} that appears in Eq. (1) was estimated using the Maxwell's model [22]:

$$k_{\mathrm{eff}} = k_m \frac{k_d + 2k_m + 2\phi(k_d - k_m)}{k_d + 2k_m - \phi(k_d - k_m)}. \tag{2}$$

where k_d is the thermal conductivity of the dispersed PCM as given by Eq. 5 and k_m corresponds to average value of the thermal conductivity for the whole matrix.

The finite volume method is used to resolve Eq. (1). Thus, the thickness of the wall is divided into N control volumes of gradual increasing size $\{V_i, i = 1 \rightarrow N\}$ (from the boundary to the center). The number of inclusions in a control volume is [23]:

$$\Lambda_i = \frac{6\phi V_i}{\pi d^3} \tag{3}$$

where d stands for the diameter of the spheres.

The Λ_i spheres in each control volume are identical and are supposed to follow the same thermal or phase change process, thus, a unique sphere is modeled per control volume, representing the kinetics of the other spheres. The "enthalpy" finite volume method is used to model the heat transfer with phase change within the N different spheres. This method is based on an enthalpy formulation of the heat equation (used here in its temperature form) applied to both liquid and solid phases. Thus, a unique mesh (or grid) cover the two media (liquid and solid). The kinetics of the phase change

(freezing or melting) is related to the evolution of the liquid phase fraction f of the PCM. The heat equation inside the spheres reads as:

$$\int_{v_i} (\rho c_p)_d \frac{\partial T}{\partial t} \mathrm{d}v = \int_{s_i} k_d \vec{\nabla} T \cdot \vec{\mathrm{d}}s - \int_{v_i} \rho_d L_m \frac{\partial f}{\partial t} \mathrm{d}v \tag{4}$$

The model is unidimensional, formulated in spherical coordinates. The spheres are divided into M equal control volumes (the radius is unequally divided). v_i is the control volume delimited by the two spheres of radii r_i and r_{i-1}. Only the central volume ($i = 0$) has a spherical shape. The last term of Eq. (4) accounts for the evolution of the local liquid fraction in the control volume v_i. The properties Ψ (density, thermal conductivity and specific heat) of the dispersed PCM are calculated as:

$$\Psi_d = f \Psi_{\mathrm{MCP}}^{\mathrm{liquid}} + (1 - f) \Psi_{\mathrm{MCP}}^{\mathrm{solid}}. \tag{5}$$

The boundary condition for this model is of Dirichlet type at the sphere surface, i.e. the instantaneous temperature of the control volume of the composite board containing the sphere is imposed at the outer surface of this sphere. In the other hand, two types of boundary conditions are applied to the wall. At one side of the composite board ($x = 0$), a generic unsteady boundary condition is applied. Considering the diversity of possible external conditions (external convection and radiative exchanges), a sinusoidal evolution of the external wall temperature is imposed. This behaviour is representative of what is experimentally observed for example by Ismail and Castro (see Fig. 17 of [13]) and is expressed as:

$$T(x = 0, t) = \bar{T} - A \sin(2\pi\ t/\tau) \quad \text{with } \tau = 1 \text{ day}. \tag{6}$$

At the other side of the board ($x = L$), a steady convective boundary condition is applied with a heat transfer coefficient $h = 10\ W/m^2\ ^\circ\mathrm{C}$:

$$k_{\mathrm{eff}} \left. \frac{\partial T}{\partial x} \right|_L = h[T_\infty - T(L, t)] \quad \text{at } x = L. \tag{7}$$

This condition is a simplified representation of the behavior of an indoor medium maintained at a fixed temperature T_∞ by an air conditioning system for example (heating and/or cooling).

2.2. Numerical algorithms

In the scope of the present study, the supercooling phenomenon is neglected and the PCM is considered as a pure material melting at a fixed temperature T_m. This assumption can be justified by the fact that low degrees of supercooling are obtained for slow cooling rates [24] as it is the case for daily periodically changing temperatures. Furthermore, the addition of nucleating agent in the PCM can reduce the degree of supercooling which is crucial for the heat storage application. Thus, the phase change front is modeled as a thin interface (1 grid cell having $0 < f < 1$). The modeling of the progression of this front coupled to the update of the liquid fraction field f is achieved using the "new source" algorithm of Voller [25]. The field of f is updated iteratively within each time step [26], in this way, the updated value of f_i^{k+1} at iteration $k+1$ and control volume i is calculated as follows:

$$f_i^{k+1} = f_i^k + \frac{dt\ a_i^k}{\rho L_m v_i}(T_i - T_m), \tag{8}$$

where a_i^k is the coefficient of T_i in the discretized version of Eq. (4). This update is followed by an overshoot/undershoot correction:

$$f_i^{k+1} = \begin{cases} 0 & \text{if } f_i^{k+1} < 0 \\ 1 & \text{if } f_i^{k+1} > 1. \end{cases} \tag{9}$$

To easily ensure that the temperature at the phase change front is equal to the melting temperature T_m, the energy equation is penalized at the computational cells belonging to the phase change front ($0 < f_i < 1$). This procedure is performed by adding a penalization source term, equal to $10^9 \times T_m$, to the RHS term of energy equations corresponding to these cells. This practice accelerates the convergence of the f updating algorithm, and the number of iterations needed to reach convergence ($|f_i^{k+1} - f_i^k| < \varepsilon_f$) may be lowered to 2 or even 1 depending on the size of the mesh and the time-step value. The value of the tolerance ε_f was fixed to 10^{-4}.

The spatial discretization of Eqs.(1) and (4) relies on centered difference schemes with second order accuracy, while the time scheme is implicit and first order. The Thomas algorithm is used to resolve the resulting tridiagonal linear system. The time step size dt has to be sufficiently small $dt \lesssim 10^{-3}\ s$ to ensure a strong coupling between the two models (matrix and spheres models). For the different configurations (different board thicknesses L, different PCM fractions ϕ), sufficiently fine grids were used to ensure the

grid independence of the results. These values were chosen after the mesh size and time step dependency studies presented in the next section. Thus, a wall of thickness $L = 5cm$ was typically divided into $N = 80$ control volumes, while $M = 20$ was used for the spheres. Initially, the whole composite material was considered at a uniform temperature slightly higher than T_m, thus the whole PCM was at the liquid state $f = 1$.

The coupling algorithm between the different models (the board and sphere models) proceeds as follows:

Step 1: At each time step, the N phase change models (sphere models, Eq. 4) are advanced in time for a duration of dt.

Step 2: The heat flux at the spheres surface is calculated as:

$$\varphi_i = k_d \left.\frac{\partial T}{\partial r}\right|_{r=d/2} \tag{10}$$

Step 3: Φ_i, the source term of Eq. (1), is then calculated as:

$$\Phi_i = \Lambda_i \varphi_i (\pi d^2). \tag{11}$$

Step 4: Eq. (1) is then resolved for the same time step and the new temperatures of the N control volumes are obtained. These temperatures will be used as the new boundary conditions for the next time step (**Step 1**).

This loop cycle is repeated until convergence is reached.

2.3. Consistency test, mesh size dependency study and model validation

The model described above takes into account intrinsically both latent and sensible heat of the PCM. To check its consistency, the following test calculation was carried out: a wall containing $\phi = 20$ % of spherical inclusions, having the same properties as those of the matrix, is considered and its thermal behavior is compared to that of a solid wall ($\phi = 0$). Both simulations should yield exactly the same results. The thickness of the wall is $L = 50$ mm, its properties are those listed in Table 2 and the indoor conditions are the same as in section 3.1. When the temperature of the left boundary varied over time according to Eq. (6), but without crossing the melting temperature of the PCM, (which was modified for this purpose to avoid phase change: $T_m = 0$ °C for example), a

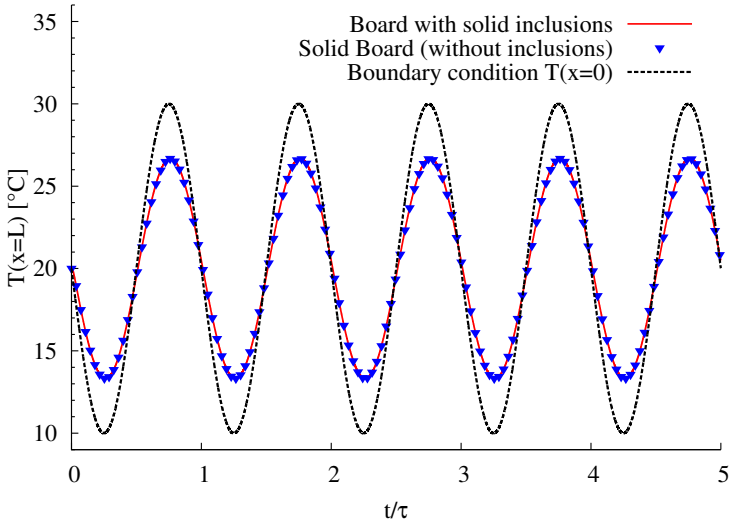

Figure 2: *Test of the model implementation: temperature evolutions at the inner boundary ($x = L$) of a solid wall with and without inclusions. The inclusions have the same properties as the matrix and do not undergo change phase. The temperature of the outer surface ($x = 0$) is also shown (Eq. 6). τ corresponds to one day.*

perfect match between the results from the two configurations is observed (see Fig. 2). As expected, the spheres behave as parts of a homogeneous material.

The choice of the adequate mesh size for the two models (board and sphere), representing the best compromise between accuracy and computation cost, has been done after three series of computations, where the N, M and dt parameters have been progressively varied. An example of results provided by such a procedure is given in Fig. 3, for the case of the parameter N (the number of computational cells within the board thickness) and for a board thickness of $L = 2.5$ cm. N was varied from 20 to 60. Qualitatively speaking, the global behavior proves to be the same for all the mesh sizes. Quantitatively, the results on the coarser grids converge rapidly to the values obtained by the finest one ($N = 60$), while the relative difference between the values obtained for $N = 60$ and $N = 40$ is always below 5 %. Thus, the value $N = 40$ was selected. Fig. 4 shows the results of a time step dependency study. A reasonable choice corresponds to $dt = 10^{-3}s$ since for a larger value of $dt = 10^{-2}s$ parasite oscillations began to appear. A similar analysis (not detailed here) allowed us to choose $M = 20$.

The two parts of the implemented model were validated separately since no reference solution is available (to the authors knowledge) for a system of mono-dispersed PCM

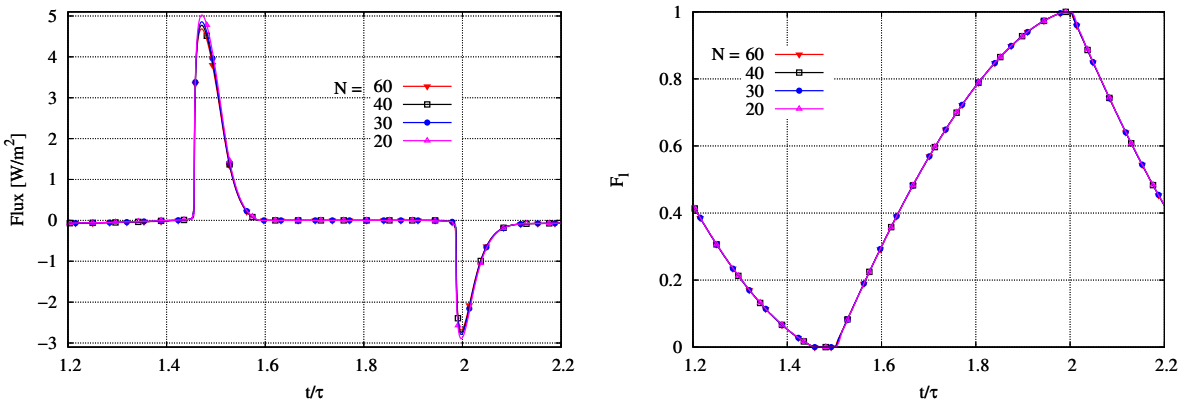

(a) Internal heat flux **(b)** Total liquid fraction

Figure 3: *Results obtained for different mesh sizes N of the composite board model with $L = 25$ mm and $\phi = 20$ % ($M = 20$).*

spheres in a matrix. Thus, the unsteady model of heat conduction through a board was compared successfully to the classical 1D analytical solution, while the sphere phase change model was validated against reference solutions given in the literature. Yang and Zhao [27] proposed a solution to the spherical Stefan problem during solidification. A finite difference approach combined with explicit and implicit Euler time integration was developed to solve the Stefan problem involving liquid–solid moving interfaces. The non-linearities introduced by the moving boundary were simplified by the use of a convenient transformation of dimensionless variables.

They compared their results to those obtained using the iterative analytical series solution of Davis and Hill [28], which is an approximate analytical solution. As an example, it is possible to compare in Tab.1 the present results with those of Refs. [27] and [28]. The selected quantity represents the number of days t/τ necessary to reach a complete solidification. It has been obtained for a mesh of $M = 20$ and for different values of the Stefan number (Ste). The agreement is quite good.

3. Results

3.1. Effect of board thickness and PCM amount

The composite considered in this study consists of a solid matrix formed by a thermally insulating material containing a dispersed paraffin PCM. The properties of the matrix material and of the PCM are given in Table 2. Monodisperse spherical PCM are considered

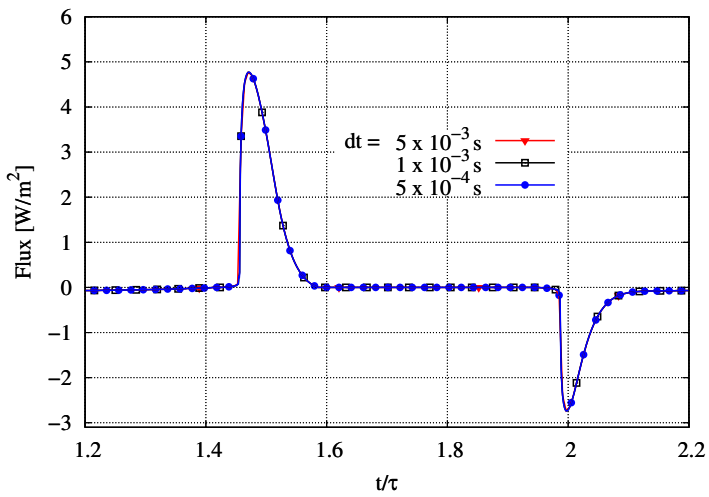

Figure 4: *Internal heat flux obtained with different time step values dt for a board of $L = 25$ mm and $\phi = 20$ % ($N = 40$; $M = 20$).*

with a diameter $d = 100$ μm. The selected values of L are 10, 15, 20, 25, 30 and 50 mm and the considered values of the fraction of PCM ϕ range from 0 to 50 %. Simulations represent a total observation time of five days (5τ).

In this section, the mean external temperature $\bar{T}$ of Eq. (6) is taken equal to the melting temperature $\bar{T} = T_m = 20$ °C and the amplitude fixed to $A = 10$ °C (i.e. $T(0,t)$ oscillating between 10 and 30 °C). This simplified signal is chosen so as to limit the number of parameters of the study (no difference between the mean temperature and the melting temperature. Usually, the meting point of the phase change material is chosen in order to match with the average temperature of the climate zone considered). In this section also, the indoor temperature T_∞ (Eq. 7) was taken equal to T_m as well, for the sake of simplicity i.e. to avoid the introduction of an additional parameter $(T_m - T_\infty)$ in the analysis. These simplifications help to focus on the role of ϕ and L. The importance of the gap between the different temperatures is addressed in section 3.4.

The propagation of the heat flux within the wall is hampered by both the thermal resistance of the matrix and by the solid-liquid phase change of the PCM. The temperature of the inner face of the wall $T(x = L)$ is obtained by the computation and is used to deduce the heat flux crossing this surface as:

$$\varphi(x = L) = h(T_\infty - T(x = L)) \tag{12}$$

In Fig. 5, the evolution of this quantity for four different board thicknesses L and five

Table 1: *Dimensionless time to complete solidification: our results compared to those of Refs. [27] and [28].*

Ste Number	Our Results ($M = 20$)	Yang and Zhao [27]	Davis and Hill [28]
0.01	16.8356	16.8231	16.8327
0.02	8.4932	8.4863	8.4987
0.1	1.809	1.8068	1.8272
0.2	0.9669	0.9654	0.9887
1	0.2750	0.2747	0.2970
2	0.1797	0.1797	0.1988
10	0.0871	0.0881	0.0997

Table 2: *Properties of the studied materials*

Property	k $[Wm^{-1}K^{-1}]$	ρ $[kg\ m^{-3}]$	c_p $[J\ kg^{-1}K^{-1}]$	L_m $[J\ kg^{-1}]$
Insulating matrix	0.03	900	1200	–
Liquid PCM	0.15	780	2200	2.3×10^5
Solid PCM	0.20	780	2000	–
Cement	1	2000	900	–

PCM percentages ϕ is given and compared with the case without PCM ($\phi = 0$, PCM free material). It is observed that for the thin board case $L = 10$ mm, and even for high values of ϕ, the effect of the phase change, which stops the propagation of heat towards the inside, is effective for only a short period of time, after which the flux increases rapidly and reaches values higher than that of the flux of the PCM free case. In fact, at the end of the phase change, the one-phase PCM (solid or liquid) has a much higher thermal conductivity than that of the matrix (see Tab.2), the effective conductivity of the composite being the more important as ϕ is higher. For thicker walls ($L = 15$ and 20 mm), the time interval during which the phase change occurs is longer, delaying the moment at which the wall becomes purely conductive and that occurs after the reversal of the external temperature signal, which limits the negative impact of the higher PCM conductivity.

Beyond $L \geqslant 25$ mm and for some values of ϕ ($\geqslant 20\%$), the phase change process remains incomplete during a whole cycle and along the wall thickness. As a consequence, no heat flux crosses the wall during the whole process. The presence within the wall of a

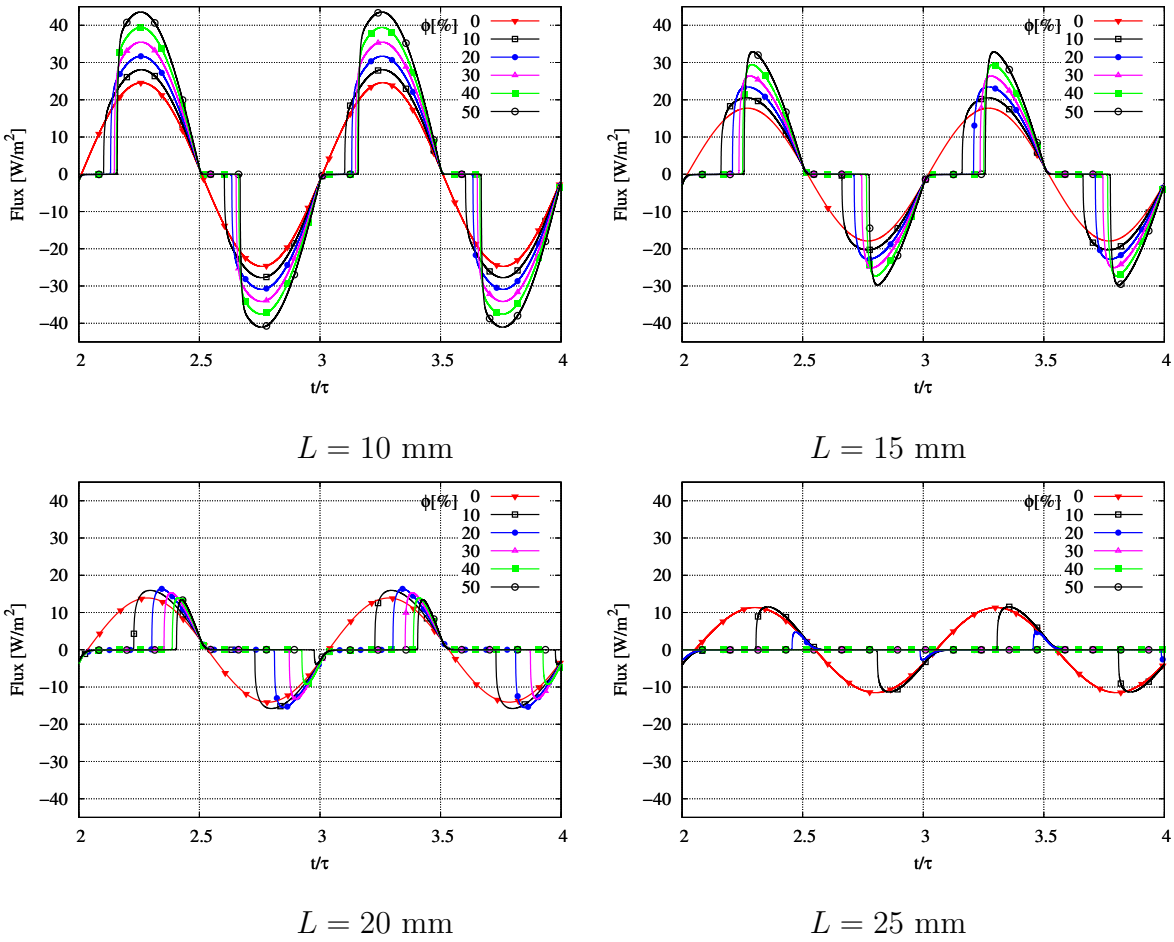

Figure 5: *Heat flux crossing walls of thickness equal to 10, 15, 20 and 25 mm and with different PCM percentages ϕ.*

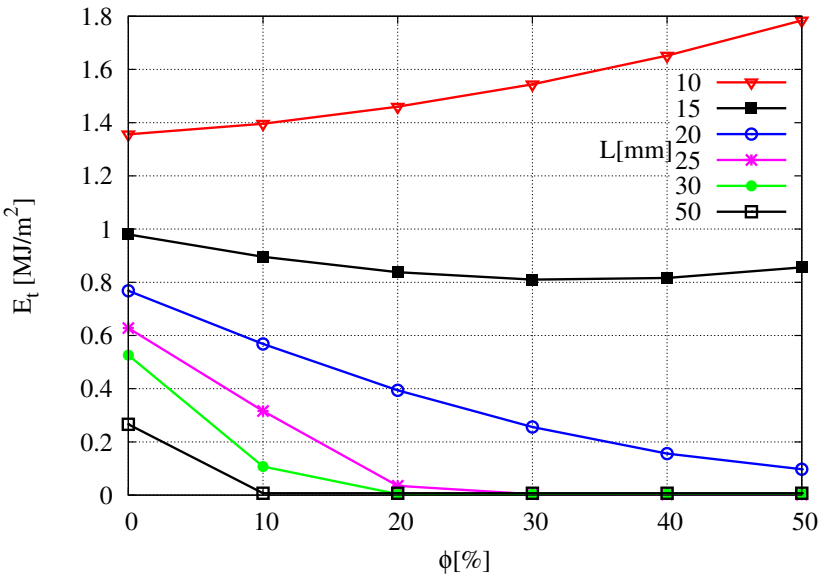

Figure 6: *Cumulative total energy (Eq. 13) crossing the indoor surface of the wall in both directions for different thicknesses and different PCM percentages.*

phase change front (i.e. a zone where the PCM spheres are in a two-phase state) acts as a thermal barrier.

In order to give a comparison of the behavior of a large number of possible (L, ϕ) combinations, a unique average quantity E_t is defined. It represents the daily total energy that crosses a unit area of the inner wall surface in both directions (averaged over a 5-day period):

$$E_t = \frac{1}{5}\int_0^{5\tau} |\varphi(x=L)|\mathrm{d}t = \frac{1}{5}\int_0^{5\tau} |h\left(T_\infty - T(x=L)\right)|\,\mathrm{d}t \tag{13}$$

Thus, E_t is the theoretical energy needed to counterbalance (by heating or cooling) the effect of heat fluxes crossing the wall. This quantity is given in Fig. 6 for a wide range of L and ϕ values. By analyzing in this figure the behavior of the $L = 10$ mm board, it can be seen that the addition of PCM to the matrix, even at a low percentage, has a negative effect on its thermal insulation behavior, since its performances for $\phi > 0$ are lower than those obtained for the PCM free case ($\phi = 0$).

For $L = 15$ mm, the addition of a percentage of PCM such as $\phi \leqslant 30\%$ has a positive effect that increases as ϕ is increased, up to a value of $\phi \simeq 30\%$. Beyond this value the insulation performances of the wall decrease, yet remaining better than those of a PCM free board. Thus, for this thickness, the addition of such a high percentage of PCM ($\phi > 30\%$) is not justified, at least for cost reasons, since better performances can be

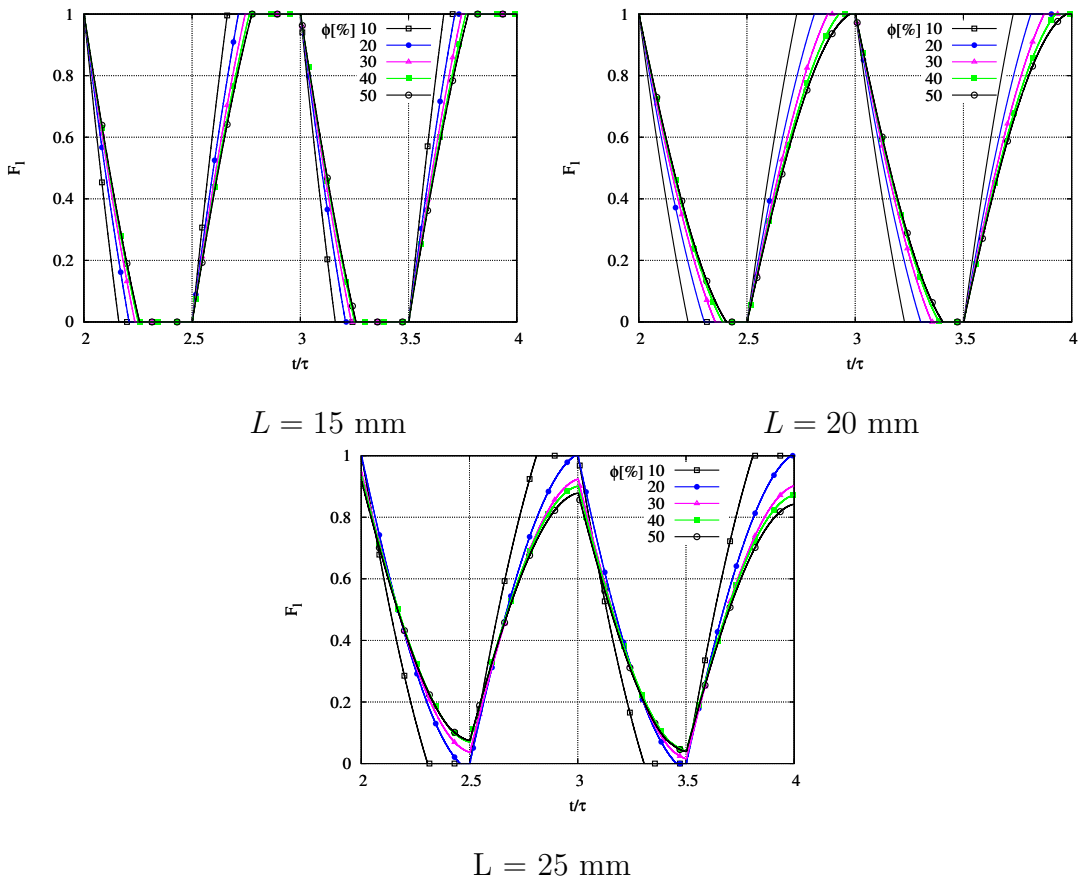

Figure 7: *Total liquid fraction of the dispersed PCM for 3 wall thicknesses L = 15, 20 and 25 mm.*

achieved by slightly increasing the thickness (see $L = 20$ mm and $\phi = 0$). The board of thickness $L = 20$ mm exhibits performances that improve continuously with the increase of the amount of PCM, but without reaching the limit of $E_t = 0$ (permanent thermal barrier). This limit is almost reached by the board of $L = 25$ mm from $\phi \geqslant 20\%$.

Actually, as seen from the curves of Fig. 7, which give the total liquid fraction of PCM of all the inclusions of the composite board, for $L = 20$ mm, complete solidification and fusion occur for all ϕ values at every cycle. On the other hand, for $L = 25$ mm and from $\phi > 20\%$, the phase change of the PCM is not complete at every cycle, which indicates the permanent presence of a two-phase zone at $T = T_m$ that sweeps through the wall thickness between $x = 0$ and L without disappearing. Therefore, it is very interesting to choose the conditions that keep as long as possible the PCM in a two-phase state. Of course, this is only possible for situations with very regular cyclic thermal loads.

For values of $L < 20$ mm (see Fig. 6), performance improvement necessarily involves an increase of the thickness L. In contrast, from $L = 20$ mm, better performances (in

comparison to a pure insulation) can be achieved with only 10 % of PCM compared to that obtained when using a 25 mm-thick PCM free board. With a PCM percentage of 40 %, the performances of a board of $L = 50$ mm of pure insulating material (i.e. PCM free) are recovered. So, in these conditions, if space-saving constraints arise, a pure insulating material can be advantageously replaced by a thinner insulating material containing a dispersed PCM.

3.2. Dispersion in a cement-based wall

The system studied in the previous section consists of the dispersion of PCM in a less conducting material (insulating material). Thus, the presence of the PCM has a positive effect as long as the phase change is in progress, since at the end of the phase change, the conductivity of the composite material becomes higher than that of the matrix material. Hence, it is interesting to compare this behavior to the one of a more frequently used system that consists of the dispersion of the PCM within a higher thermal conducting building material such as a mortar or a cement wall [29]. For this purpose, numerical experimentations were conducted concerning such a wall by replacing the thermophysical properties of the insulating matrix by those of a typical cement material exhibiting higher thermal conductivity (see Tab. 2). Fig. 8 gives the evolution of the heat flux at internal wall surface and of the global liquid fraction for two wall thicknesses and different percentages of PCM.

The addition of PCM to this cement wall has a positive effect on the reduction of the heat flux crossing the wall whatever the percentage and the wall thickness. Obviously, the more PCM is added the more pronounced is this effect. Since the PCM conductivity is below that of the cement, there is no inversion of the effect after the end of the phase change process, as it is the case for the insulation matrix (see Fig. 5). However, contrarily to an insulating material, the dispersion of PCM in a cement wall implies that aspects of material strength should be examined, because these types of material are usually used in the structure. The non inversion of the effect of PCM inclusion, can also be obtained for other building materials such as gypsum boards since their thermal conductivity is comparable to that of PCM.

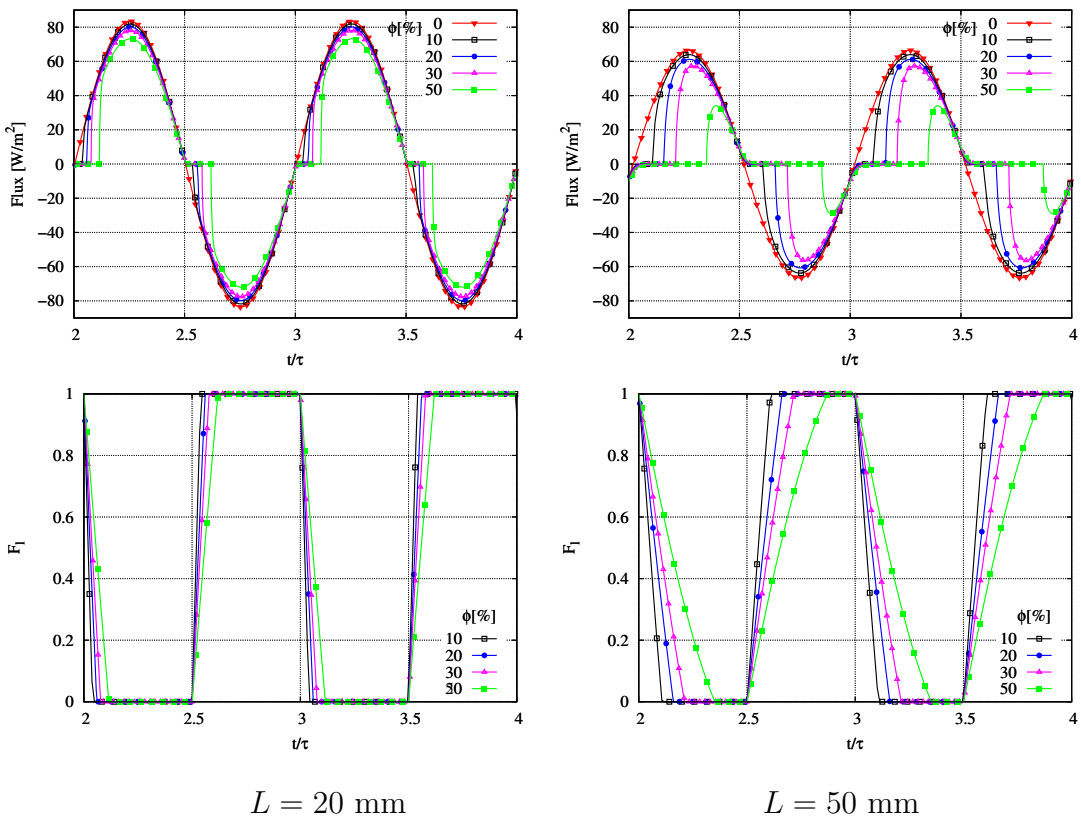

Figure 8: *Heat flux (top) crossing a cement wall and total liquid fraction (bottom) of the dispersed PCM for wall thicknesses of 20 and 50 mm with different PCM percentages ϕ.*

3.3. Effect of small scale stochastic fluctuations of the external temperature

The results presented above were obtained for a smooth sinusoidal variation of the external temperature boundary condition. In the following, the sensitivity of these results to the presence of small fluctuations of the external temperature signal is examined. These fluctuations are supposed to mimick the indirect effects that external conditions modifications (clouds passage or/and wind speed and direction fluctuations for example) could exert on the external wall temperature. To that end, the temperature signal $T(t)$ is expressed as the sum of three terms $T(t) = \bar{T} + T'_p(t) + T'_s(t)$, with $\bar{T}$ being the temporal mean value, T'_p the periodic (sinusoidal) variation and T'_s a stochastic fluctuation. The last one is obtained by resolving a stochastic differential equation of the Langevin's type [30], that writes as:

$$\mathrm{d}T'_s(t) = \frac{-T'_s(t)\mathrm{d}t}{\Lambda_T} + \sigma_{T'_s}\sqrt{\frac{2}{\Lambda_T}}\mathrm{d}W_t \tag{14}$$

where W_t represents a Wiener's process. The initial condition $T'_s(0)$ is chosen as a Gaussian random variable having a zero mean value and a variance $\sigma^2_{T'_s}$. The numerical solution of

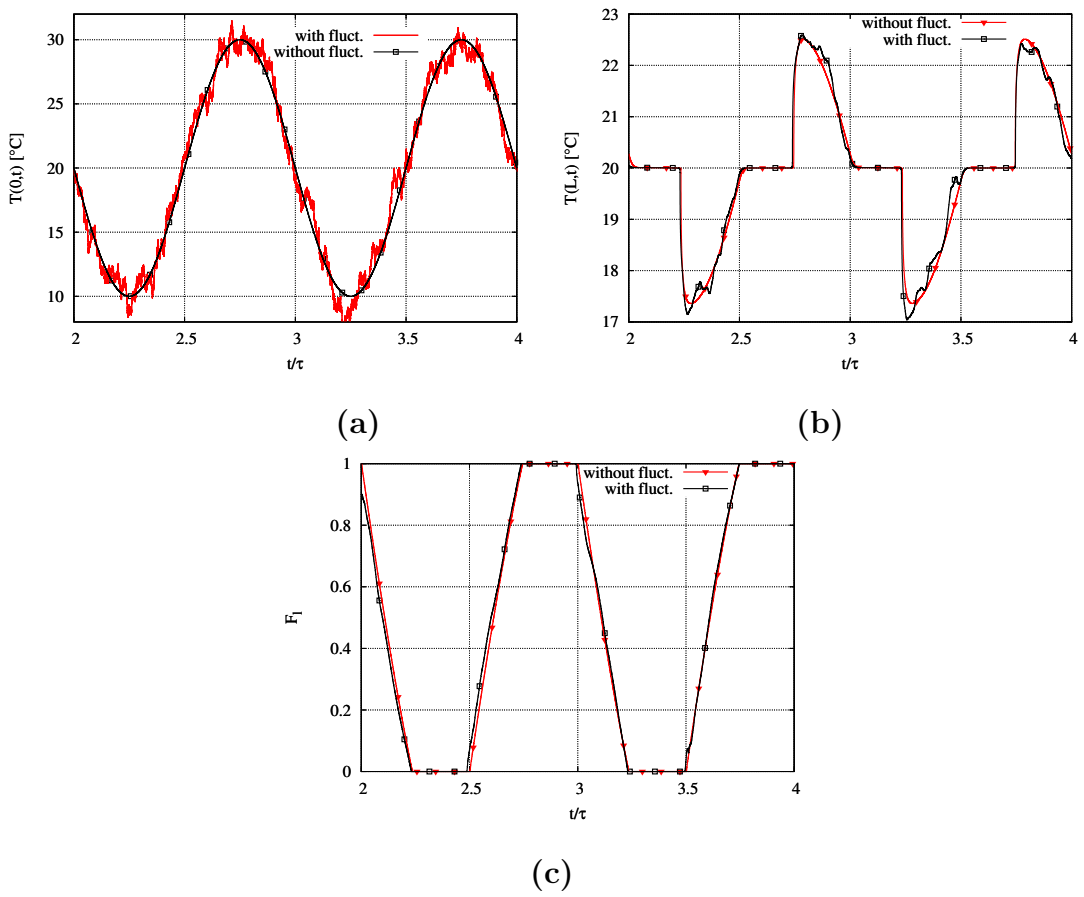

Figure 9: *The external temperature signal with superimposed small scale stochastic fluctuations (a), time evolution of the corresponding temperature at the inner surface $x = L$ for a board of thickness $L = 15$ mm and for $\phi = 30$ % (b) and the evolution of the total liquid fraction (c). The case of an insulating matrix is considered here.*

these equation is obtained using the "*hybrid*" method [31] given as:

$$T_s'(t+\Delta t) = exp\left(-\frac{\Delta t}{\Lambda_T}\right) T_s'(t) + \sigma_{T_s'}\sqrt{1 - exp\left(-\frac{2\Delta t}{\Lambda_T}\right)}\omega(t) \tag{15}$$

where $\omega(t)$ denotes an independent random normal variable of zero mean value and variance unity i.e. $\omega(t) \in N(0,1)$. Following Wilson and Zhuang [32], the choice of $\Delta t = \frac{\Lambda_T}{10}$ leads to a discrepancy error less than 2 % when compared to the theoretical Gaussian probability density function of T_s'.

Fig. 9 displays the signal obtained by the above-mentioned method for the parameters $\Lambda_T = 1800$ s (an integral time scale representative for instance of that of the passage of clouds) and $\sigma_{T_s'} = 0.9$ (representing the rms amplitude of the fluctuations) and gives the temperature evolution at the inner surface of the wall obtained when the signal is applied as an external boundary condition.

It is clear that for the conditions considered, the sensitivity of the thermal behavior of the board to the presence of small-scale fluctuations in the outside temperature is relatively weak, and its impact on both temporal variation of inner wall temperature ($x = L$) and total liquid fraction F_l is marginal.

Thus, subject to confirmation of the relevance of the generated fluctuations, these results indicate that using a purely harmonic outside temperature signal is sufficient to account for the dynamics of the thermal behavior of the wall.

3.4. Effect of seasonal weather (winter/summer)

Using a composite board as an insulation implies that this material is integrated to a wall or a building envelope on a yearly basis, and as a consequence, its integration should lead to an overall positive budget over the passing seasons. Thus, the choice of the melting temperature of the PCM has a crucial importance. In this study, the question put forward is the following: "For which conditions is it interesting to replace a pure insulation board (i.e. PCM free) by a PCM-composite one having the same thickness ?". So, the question is not about the relevance of superimposing an additional PCM-composite board to a wall. Furthermore, the question of the cost of materials is not addressed, only the energetic point of view is dealt with.

In the present study, the thermal behavior of a PCM-free material and that of a composite one are compared during two typical days representing summer and winter seasons, respectively. The corresponding external temperature variations were taken as:

$$\text{Summer:} \quad T(x = 0, t) = 27 - 7\sin(2\pi\ t/\tau) \quad [^\circ\text{C}] \tag{16}$$

$$\text{Winter:} \quad T(x = 0, t) = 5 - 7\sin(2\pi\ t/\tau) \quad [^\circ\text{C}] \tag{17}$$

Thus, the same amplitude is taken for the two signals (7 °C) while the mean temperatures are 27 °C and 5 °C for summer and winter days, respectively. The indoor temperatures was chosen to be 26 °C and 20 °C which are close to the standard settings for HVAC systems for summer and winter seasons. We note that contrarily to the previous sections, the mean temperatures are here different from the indoor temperatures, particularly for the winter day. The gap with the melting temperature is analyzed here by studying the behavior of PCMs having different T_m temperatures. This analysis was done for a unique board ($L = 25$ mm and $\phi = 20$ %) whose characteristics were chosen

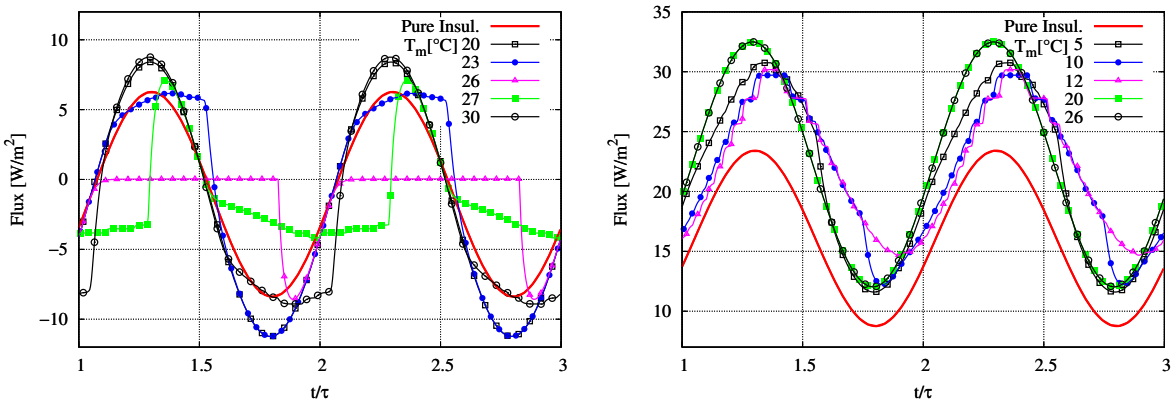

(a) Summer day **(b)** Winter day

Figure 10: *Heat flux crossing the internal surface of a board (L = 25 mm, ϕ = 20 %) with PCMs of different T_m and during typical summer and winter days.*

using the results of Fig. 6. Thus, the selected board has the minimal L and ϕ values that yield an almost null crossing energy E_t.

The results presented in Fig. 10 give the time evolution of the heat flux crossing the indoor side of the board for the two typical days considered. For the summer day, the melting temperatures are ranging from 20 to 30 °C and the results are compared to the case of a PCM free material ($\phi = 0$ %). The whole crossing energies per day E_t (Eq. 13) are summarised in Fig. 11(a). In these figures, it can be noticed that the case of $T_m = 26$ °C (equal to the indoor target temperature) gives the best results, while the case $T_m = 27$ °C (equal to the mean external temperature) behaves worse but remains better than all other T_m values, whose results are even worse than those obtained with the PCM free board ($\phi = 0$ %, Fig. 11(a)). In Fig. 12(a), that gives the total liquid fraction of the PCM, it is observed that for $T_m = 26$ °C and 27 °C comparable amounts of PCM were solidified/melted respectively (but larger compared to the other PCMs). It is clear that the best choice for T_m is to be as close as possible to the indoor temperature to maintain most of the time in the board a uniform temperature zone ($\simeq T_m$), located between the melting front and the internal surface, that will be limiting the heat flux.

For the winter day, none of the T_m choices ranging from 5 to 26 °C perform better than the PCM free counterpart. All the global results are comparable (Fig. 11(b)) for all the PCMs, with a slight advantage though for lower melting temperatures. Thus, even if the phase change process takes place within the board (Fig. 12(b)), the temperature

gradient is sufficiently high to generate a more important heat flux related to the higher conductivity of the PCM-composite.

Even if it is clearly not relevant for a winter weather, the value $T_m = 26$ °C has been retained to have a global overview of the annual behavior of the insulating wall. It appears that the addition of PCM to an insulating matrix permits to save 2.9×10^5 J/m^2 per summer day, while it causes a loss of 5.34×10^5 J/m^2 per winter day. Thus, in order to have an annual positive budget, compared to a PCM free insulation, this board should be used in hot climatic zones featuring more summer-like days than winter ones. Results with similar trends have been reported by Izquierdo-Barrientos et al. [18] and Ye et al. [33].

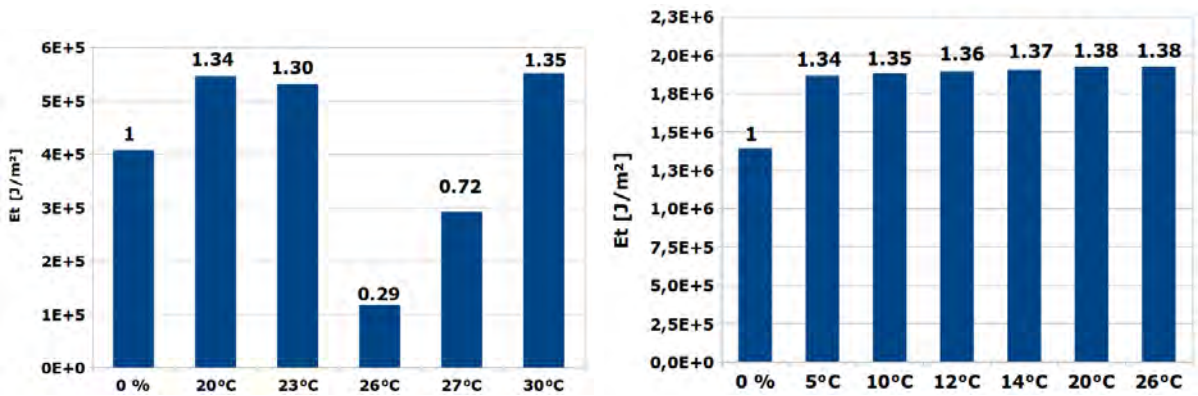

(a) Summer day **(b)** Winter day

Figure 11: *Cumulative total energy E_t (Eq. 13) crossing the indoor surface of the board in both directions for typical summer and winter days and for different T_m ($L = 25$ mm, $\phi = 20$ %). The values over the bars are the ratios $E_t/E_t(\phi = 0\%)$ that give a comparison to the PCM free case.*

4. Conclusion

In this study, the thermal behavior of a composite material consisting of a micro-dispersed PCM in an insulating polymer matrix is analyzed. The targeted application is the thermal insulation and a gain of thermal inertia of a building envelope. By using two coupled finite volume models, the behavior of the composite board was studied when submitted to a cyclic harmonic thermal excitation. Different board thicknesses (L) were considered as well as various volume percentages of PCM inclusions (ϕ). It has been observed that for a thin board, the introduction of PCM has a negative effect on its behavior, as it increases its overall thermal conductivity. It was also shown that with

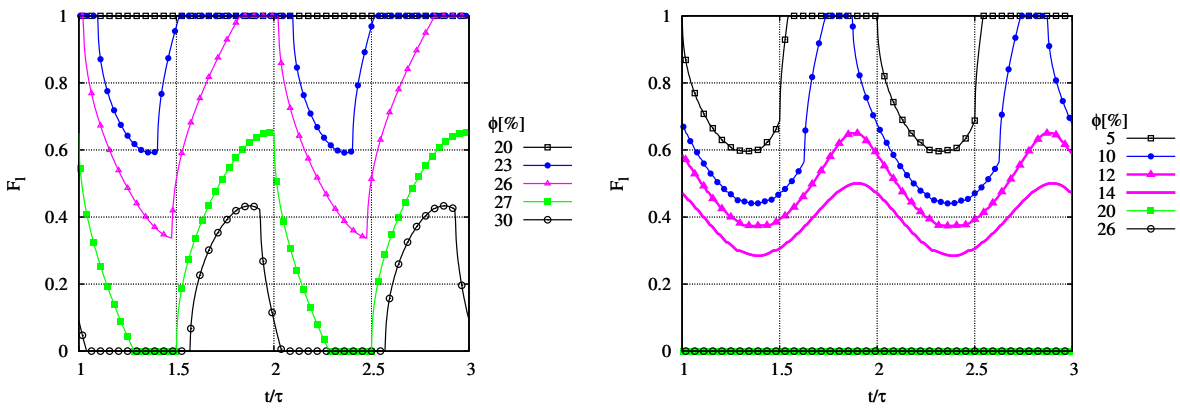

(a) Summer day **(b)** Winter day

Figure 12: *Total liquid fraction of PCM inside a board ($L = 25$ mm, $\phi = 20$ %) with PCMs of different melting temperatures T_m and during typical summer and winter days.*

some combinations of L and ϕ, it is possible to durably maintain an active phase change front within the board which then behaves as a genuine thermal barrier. To date, this feature is not commonly reported. Indeed, it is usually considered that the effectiveness of the system may be considerably reduced if the PCM is not able to completely solidify or melt. The results also revealed how pure insulating boards could be favorably replaced by thinner boards enriched with micro-dispersed PCM allowing the reduction of the overall thickness of the insulation. It was also shown that the temperature variations within the material are weakly sensitive to the presence of small scale fluctuations of the external temperature, representing transient climatic variations. We confirmed also that replacing a pure insulation (i.e. PCM free) by a PCM-composite insulation should be studied with care on a yearly basis, since a well behaving material in summer may be a very poor choice during winter. Thus, the PCM-composite board should be optimized (thickness, % of PCM, melting temperature, thermal properties of the matrix) taking into account the climate in which the building is located and the internal and external heat loads.

5. References

[1] S. A. Memon. Phase change materials integrated in building walls: A state of the art review. *Renewable and Sustainable Energy Reviews*, 31:870–906, 2014.

[2] J. Kosny, A. Fallahi, N. Shukla, E. Kossecka, and R. Ahbari. Thermal load mitigation

and passive cooling in residential attics containing PCM-enhanced insulations. *Solar Energy*, 108:164–177, 2014.

[3] S.E. Kalnæs and B.P. Jelle. Phase change materials and products for building applications: A state-of-the-art review and future research opportunities. *Energy and Buildings*, 94:150–176, 2015.

[4] Y. Zhang, G. Zhou, K. Lin, Q. Zhang, and H. Di. Application of latent heat thermal energy storage in buildings: State-of-the-art and outlook. *Building and Environment*, 42(6):2197–2209, 2007.

[5] V.V. Tyagi and D. Buddhi. PCM thermal storage in buildings: a state of art. *Renewable and Sustainable Energy Reviews*, 11(6):1146–1166, 2007.

[6] N. Soares, J.J. Costa, A.R. Gaspar, and P. Santos. Review of passive PCM latent heat thermal energy storage systems towards buildings' energy efficiency. *Energy and Buildings*, 59:82–103, 2013.

[7] F. Kuznik, D. David, K. Johannes, and J.-J. Roux. A review on phase change materials integrated in building walls. *Renewable and Sustainable Energy Reviews*, 15(1):379–391, 2011.

[8] M.A. Medina, J.B. King, and Zhang M. On the heat transfer rate reduction of structural insulated panels (SIPs) outfitted with phase change materials (PCMs). *Energy*, pages 667–678, 2008.

[9] F. Ascione, N. Bianco, R.F. De Masi, F. de'Rossi, and G.P. Vanoli. Energy refurbishment of existing buildings through the use of phase change materials: energy savings and indoor comfort in the cooling season. *Applied Energy*, 113:990–1007, 2014.

[10] C. Castellón, M. Medrano, J. Roca, L.F. Cabeza, M.E. Navarro, A. Fernández, A.I.and Lázaro, and B. Zalba. Effect of microencapsulated phase change material in sandwich panels. *Renewable Energy*, 35(10):2370–2374, 2015.

[11] V.V. Tyagi, S.C. Kaushik, S.K. Tyagi, and T. Akiyama. Development of phase change materials based microencapsulated technology for buildings: A review. *Renewable and Sustainable Energy Reviews*, 15(2):1373–1391, 2011.

[12] T. Khadiran, M.Z. Hussein, Z. Zainal, and R. Rusli. Encapsulation techniques for organic phase change materials as thermal energy storage medium: A review. *Solar Energy Materials and Solar Cells*, 143(7803):78–98, 2015.

[13] K.A.R. Ismail and J.N.C. Castro. PCM thermal insulation in buildings. *International journal of energy research*, 21(14):1281–1296, 1997.

[14] M. Ahmad, A. Bontemps, H. Sallée, and D. Quenard. Experimental investigation and computer simulation of thermal behaviour of wallboards containing a phase change material. *Energy and Buildings*, 38(4):357–366, 2006.

[15] F. Kuznik and J. Virgone. Experimental assessment of a phase change material for wall building use. *Applied Energy*, 86(10):2038–2046, 2009.

[16] A. Castell, I. Martorell, M. Medrano, G. Perez, and L.F. Cabeza. Experimental study of using PCM in brick constructive solutions for passive cooling. *Energy and Buildings*, 42(4):534–540, 2010.

[17] J. Kosny, E. Kossecka, A. Brzezinski, A. Tleoubaev, and D. Yarbrough. Dynamic thermal performance analysis of fiber insulations containing bio-based phase change materials (PCMs). *Energy and Buildings*, 52:122–131, 2012.

[18] M.A. Izquierdo-Barrientos, J.F. Belmonte, D. Rodríguez-Sánchez, A.E. Molina, and J.A. Almendros-Ibáñez. A numerical study of external building walls containing phase change materials (PCM). *Applied Thermal Engineering*, 47:73–85, 2012.

[19] L. Cao, D. Su, Y. Tang, G. Fang, and F. Tang. Properties evaluation and applications of thermal energy storage materials in buildings. *Renewable and Sustainable Energy Reviews*, 48:500–522, 2015.

[20] S. Caubet, Y. Le Guer, B. Grassl, K. El Omari, and E. Normandin. A low-energy emulsification batch mixer for concentrated oil-in-water emulsions. *AIChE Journal*, 57(1):27–39, 2011.

[21] C. Forgacz, S. Caubet, Y. Le Guer, B. Grassl, K. El Omari, M. Birot, and H. Deleuze. Synthesis of porous emulsion-templated monoliths using a low-energy emulsification batch mixer. *Journal of Polymers and the Environment*, 21(3):683–691, 2013.

[22] D.J. Jeffrey. Conduction through a random suspension of spheres. *Proc. R. Soc. Lond. A*, 335:355–367, 1973.

[23] A. M. Thiele, A. Kumar, G. Sant, and L. Pilon. Effective thermal conductivity of three-component composites containing spherical capsules. *International Journal of Heat and Mass Transfer*, 73:177–185, 2014.

[24] X. Zhang, Y. Fan, X. Tao, and K. Yick. Crystallization and prevention of supercooling of microencapsulated n-alkanes. *Journal of Colloid and Interface Science*, 281(2):299–306, 2005.

[25] V.R. Voller. Fast implicit finite-difference method for the analysis of phase change problems. *Numerical Heat Transfer Part B-Fundamentals*, 17:155–169, 1990.

[26] K. El Omari, T. Kousksou, and Y. Le Guer. Impact of shape of container on natural convection and melting inside enclosures used for passive cooling of electronic devices. *Applied Thermal Engineering*, 31:3022–3035, 2011.

[27] J. Yang and C.Y. Zhao. Solidification analysis of a single particle with encapsulated phase change materials. *Applied Thermal Engineering*, 51(1):338–346, 2013.

[28] G.B. Davis and J.M. Hill. A moving boundary problem for the sphere. *IMA Journal of Applied Mathematics*, 29(1):99–111, 1982.

[29] L.F. Cabeza, C. Castellón, M. Nogués, M. Medrano, Leppers R., and O. Zubillaga. Use of microencapsulated PCM in concrete walls for energy savings. *Energy and Buildings*, 39(39):113–119, 2007.

[30] T. Kousksou and P. Bruel. Encapsulated phase change material under cyclic pulsed heat load. *International Journal of Refrigeration*, 33(8):1648–1656, 2010.

[31] G.C. Crone. *Parallel Lagrangian models for turbulent transport and chemistry*. PhD thesis, University of Utrecht, 1997.

[32] J.D. Wilson and Y. Zhuang. Restriction on the timestep to be used in stochastic lagrangian models of turbulent dispersion. *Boundary-Layer Meteorology*, 49(3):309–316, 1989.

[33] H. Ye, L. Long, H. Zhang, and R. Zou. The performance evaluation of shape-stabilized phase change materials in building applications using energy saving index. *Applied Energy*, 113:1118–1126, 2014.

Nomenclature

A	Temperature amplitude (K)
c_p	Specific heat ($J\ kg^{-1}K^{-1}$)
d	PCM inclusions diameter (m)
dt	Integration time step (s)
f	Local liquid fraction of PCM
h	Heat transfer coefficient ($W.m^{-2}.K^{-1}$)
k	Thermal conductivity ($W.m^{-1}.K^{-1}$)
L	Board thickness (m)
L_m	PCM latent heat of melting ($J.kg^{-1}$)
N	Number of control volumes (Matrix discretization)
M	Number of control volumes (PCM inclusion discretization)
r	Radial coordinate in a PCM inclusion (m)
S	V control volume boundary
Ste	Stefan number $= c_p \Delta T / L_m$
s	v control volume boundary
t	Time (s)
T	Temperature (K)
$\overline{T}$	Time averaged temperature (K)
T'	Temperature fluctuation (K)
v	Control volume (PCM inclusion discretization)
V	Control volume (Matrix discretization)
W_t	Wiener process
x	Spatial coordinate normal to the board (m)
Greek symbols	
ϵ_f	Convergence parameter
Λ_i	Number of PCM inclusions in V_i
Λ_T	Integral time scale (s)

φ	Heat flux ($W.m^{-2}$)
ϕ	PCM volumic fraction
Φ	Source term
ρ	Density ($kg.m^{-3}$)
σ	Standard deviation of the stochastic signal
τ	One-day period
Subscripts	
d	Relative to the dispersed PCM
eff	Effective
i	Control volume index
m	Melting
p	Periodic
s	Stochastic
∞	Relative to indoor conditions
Superscripts	
k	Iteration index
Acronym	
PCM	Phase change material